

## Laser Photoexcitation of NAD(P)H Induces Reduction of P450 BM3 Heme Domain on the Microsecond Time Scale

Hazel M. Girvan, Derren J. Heyes, Nigel S. Scrutton, and Andrew W. Munro\*

Contribution from the Manchester Interdisciplinary Biocentre, Faculty of Life Sciences, University of Manchester, 131 Princess Street, Manchester M1 7DN, U.K.

Received February 26, 2007; E-mail: Andrew.Munro@Manchester.ac.uk

**Abstract:** We demonstrate that photoexcitation of NAD(P)H at 355 nm using a Nd:YAG laser leads to rapid reduction of the heme domain of the *Bacillus megaterium* fatty acid hydroxylase flavocytochrome P450 BM3. An aqueous electron derived from photoexcited NAD(P)H is rapidly transferred to the heme domain, enabling the formation of a carbon monoxide complex of the ferrous P450 ( $\text{Fe}^{\text{II}}\text{-CO}$ ) on the microsecond time scale. Using this approach we have determined the limiting rate constant ( $1770 \text{ s}^{-1}$  for substrate-free heme domain) for formation of the  $\text{Fe}^{\text{II}}\text{-CO}$  complex. We find no dependence of the observed rate of  $\text{Fe}^{\text{II}}\text{-CO}$  complex formation on NAD(P)H concentration but demonstrate a hyperbolic dependence on carbon monoxide concentration. The apparent dissociation constant for the complex of carbon monoxide bound noncovalently to the ferric form of the BM3 heme domain (and with NADH as reductant) is  $323 \mu\text{M}$ . Binding of a P450 substrate (*N*-palmitoylglycine) weakened the complex between carbon monoxide and the ferric BM3 heme domain ( $K_{\text{d}}$  increased to  $1404 \mu\text{M}$ ) but enhanced the rate of formation of the  $\text{Fe}^{\text{II}}\text{-CO}$  complex ( $3036 \text{ s}^{-1}$  for substrate-free heme domain). This study demonstrates the applicability of NAD(P)H photoexcitation as a method for rapid electron delivery to P450 enzymes and provides a new route to probing the P450 catalytic cycle and its transient intermediates.

### Introduction

The cytochromes P450 (P450s) are a superfamily of *b*-type cytochromes in which the heme iron is proximally coordinated by a conserved cysteine thiolate.<sup>1</sup> The distal position on the ferric heme iron is typically occupied by a water molecule in the resting (ferric) form of the P450. Binding of a (usually lipophilic) substrate in the active site generally leads to the displacement of the distal water and to a shift in heme iron spin-state equilibrium (from low-spin toward high-spin). This, in turn, makes the reduction potential of the heme iron more positive and can trigger electron transfer from a redox partner enzyme to initiate the redox part of the catalytic cycle.<sup>2</sup> The electron source in P450 enzymes is usually NAD(P)H. The two electrons derived from the oxidation of NAD(P)H by partner enzymes are shuttled one at a time to the P450 heme iron. These partner proteins usually contain flavin and/or iron sulfur clusters to mediate electron transfer.<sup>3</sup> In the first electron transfer to the P450 protein the heme iron is reduced to the ferrous form, which can then bind dioxygen. Delivery of the second electron to the ferrous-oxy P450 results in formation of the ferric peroxy intermediate, which is protonated to the ferric hydroperoxy species (compound 0). A second protonation step leads to the collapse of this species with formation of a water molecule and the highly reactive ferryl-oxo P450 species (compound 1). This

latter species is considered to be the major oxygenating intermediate in P450 catalysis and attacks the closely bound substrate, effecting its oxygenation (often forming a hydroxylated product).<sup>4</sup> Dissociation of the product (and rebinding of the distal water) restores the P450 to the resting state, ready for a further catalytic cycle.<sup>5</sup>

A well-known form of P450 enzymes is the ferrous-carbon monoxide ( $\text{Fe}^{\text{II}}\text{-CO}$ ) complex (Figure 1). Reduction of the heme iron to the  $\text{Fe}^{\text{II}}$  state and binding of carbon monoxide (rather than dioxygen) to the ferrous iron yields a species with a Soret spectral maximum shifted from  $\sim 418 \text{ nm}$  (the low-spin ferric heme) to  $\sim 450 \text{ nm}$  (the cysteinate-coordinated CO-bound form).<sup>6</sup> This 450 nm (pigment) species, from which the name cytochrome P450 derives, is a characteristic feature of all P450 enzymes.<sup>5</sup> One of the most widely studied P450 enzymes is flavocytochrome P450 BM3 (BM3) from the soil bacterium *Bacillus megaterium*. BM3 is a fatty acid hydroxylase comprising a diflavin (FAD- and FMN-containing) reductase redox partner fused to a heme domain in a single polypeptide.<sup>7,8</sup> The reductase is closely related to NADPH-cytochrome P450 reductase (CPR), the redox partner for the majority of mammalian P450s.<sup>9</sup> Eukaryotic CPRs are membrane-bound and

(1) Poulos, T. L.; Finzel, B. C.; Howard, A. J. *Biochemistry* **1986**, *25*, 5314–5322.

(2) Daff, S. N.; Chapman, S. K.; Turner, K. L.; Holt, R. A.; Govindaraj, S.; Poulos, T. L.; Munro, A. W. *Biochemistry* **1997**, *36*, 13816–13823.

(3) Munro, A. W.; Girvan, H. M.; McLean, K. J. *Biochim. Biophys. Acta* **2007**, *1770*, 345–359.

(4) Makris, T. M.; von Koenig, K.; Schlichting, I.; Sligar, S. G. *J. Inorg. Biochem.* **2006**, *100*, 507–518.

(5) Denisov, A. G.; Makris, T. M.; Sligar, S. G.; Schlichting, I. *Chem. Rev.* **2005**, *105*, 2253.

(6) McLean, K. J.; Warman, A. J.; Seward, H. E.; Marshall, K. R.; Cheesman, M. R.; Waterman, M. R.; Munro, A. W. *Biochemistry* **2006**, *45*, 8427–8443.

(7) Narhi, L. O.; Fulco, A. J. *J. Biol. Chem.* **1987**, *262*, 6683.

(8) Munro, A. W.; Lindsay, J. G. *Mol. Microbiol.* **1996**, *20*, 1115.

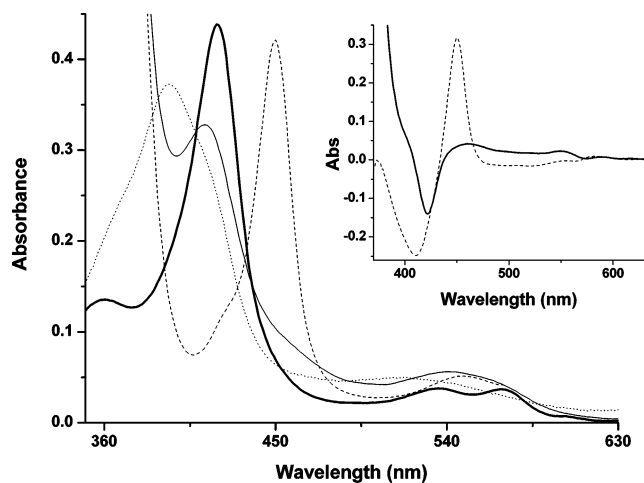


**Figure 1.** UV-vis spectral properties of the P450 BM3 heme domain. UV-vis absorption spectra are shown for the wild-type P450 BM3 heme domain ( $\sim 4.5 \mu\text{M}$ ) in various states relevant to the current study. The oxidized ( $\text{Fe}^{\text{III}}$ ) substrate-free form (thick solid line) is predominantly low-spin with its Soret peak at 418 nm and  $\alpha/\beta$  bands at 569/535 nm. The oxidized substrate (NPG)-bound form (dotted line) is predominantly high-spin with the Soret peak shifted to 394 nm and a main peak in the visible region at 521 nm. The (dithionite) reduced ( $\text{Fe}^{\text{II}}$ ) form (thin solid line) has its Soret band shifted to 412 nm with a visible region peak at 541 nm. The  $\text{Fe}^{\text{II}}$ -CO complex (dashed line) has its Soret maximum at 450 nm, with a visible region peak at 548 nm. The inset shows the difference spectra generated by subtraction of the  $\text{Fe}^{\text{II}}$  spectrum from the  $\text{Fe}^{\text{II}}$ -CO spectrum (dashed line) and by subtraction of the  $\text{Fe}^{\text{III}}$  spectrum from the  $\text{Fe}^{\text{II}}$  spectrum (solid line).

contain a lipophilic N-terminal membrane anchor.<sup>10</sup> By contrast, the CPR of BM3 is a soluble polypeptide, devoid of a membrane anchor region, and is covalently attached at the C-terminus of the fatty acid hydroxylase P450 partner protein.<sup>11</sup> BM3 has the highest rate of substrate oxygenation reported for any P450 enzyme, with arachidonic acid oxygenated at a steady-state turnover rate of  $\sim 17\,100 \text{ min}^{-1}$  at 30 °C.<sup>12</sup> Underlying this fast catalytic rate (which is  $\sim 10^3$ -fold greater than observed for many mammalian P450s) is the rapid rate of electron transfer from NADPH coenzyme to the FAD of the CPR domain and also from the FMN of the CPR domain to the P450 heme iron.<sup>13</sup> Dissection of the multidomain protein yields a functional heme-containing (P450) domain that retains its normal ability to bind substrates and ligands and which communicates with the isolated reductase domain (albeit with much slower electron-transfer rates than seen in the intact enzyme).<sup>14</sup> Trapping the enzyme in the stable ferrous CO-bound form by stopped-flow methods has been used to study electron transfer between the FMN cofactor and the P450 heme. A maximal rate ( $223 \text{ s}^{-1}$  at 25 °C) for flavin-to-heme electron transfer has been measured on mixing NADPH with myristic acid-bound BM3 in the presence of saturating CO, indicating that the first flavin-to-heme electron transfer is partially rate-limiting in catalysis.<sup>13</sup> With the use of

photoexcitation of 5-deazariboflavin to reduce protein-bound FMN cofactor, a similar rate ( $\sim 250 \text{ s}^{-1}$ ) was measured for FMN-to-heme electron transfer in a truncated form of the myristate-bound enzyme which contained only the FMN and heme domains (comprising the first 664 amino acids of the flavocytochrome).<sup>15</sup> This FMN-to-heme electron-transfer rate falls to  $\sim 18 \text{ s}^{-1}$  in the absence of myristate.<sup>15</sup> The similar rate constants obtained for FMN-to-heme electron transfer in full length and truncated forms of BM3 also emphasize the validity of studying isolated domains to obtain functional properties of these multidomain redox systems.<sup>13,15</sup>

A consequence of the relatively slow FMN-to-heme electron transfer in the BM3 enzyme is that this step is likely to be much slower than many of the subsequent steps in the P450 catalytic cycle and far slower than the rate of binding of  $\text{O}_2$  (the physiological ligand) or CO to the ferrous P450. Thus, there are technical barriers to studying the faster steps of the P450 catalytic cycle. With this in mind, we have explored alternative methods for rapidly introducing an electron directly into the heme domain using photoexcitation of nicotinamide coenzymes. We have adapted a method pioneered by Orii for rapid reduction of cytochrome *c*.<sup>16</sup> Photoexcitation of NADH releases an aqueous electron leading to near-complete reduction of cytochrome *c* within 1–2 ms.<sup>16</sup> Unlike photoexcitation studies with 5 deazariboflavin,<sup>15</sup> we demonstrate that laser photoexcitation of NAD(P)H at 355 nm leads to the direct and rapid reduction of BM3 heme. We use this method to analyze the mechanism of  $\text{Fe}^{\text{II}}$ -CO adduct formation, to determine limiting rate constants for the formation of this adduct, and to evaluate the apparent affinity for the gaseous ligand in the substrate-free and fatty acid-bound oxidized enzyme forms.

## Experimental Methods

The molecular dissection of flavocytochrome P450 BM3 into its component heme (P450) and diflavin (reductase or CPR) domains was described previously.<sup>12,14</sup> The heme domain of the enzyme (i.e., the plasmid construct encoding residues 1–472 of the 1048 amino acid protein) was expressed in *E. coli* TG1, and the P450 was purified to homogeneity as described previously.<sup>14,17</sup> Purity and integrity of the P450 were established by SDS PAGE analysis and by determination of the Soret/ $A_{280}$  ratio (the  $A_{418}/A_{280}$  ratio is typically 1.7 or more for homogeneous P450 BM3 heme domain). Heme domain was concentrated by ultrafiltration (Centriprep YM-30, Millipore) to a final concentration of approximately 1 mM, and the protein was stored at  $-80 \text{ }^\circ\text{C}$  in 50 mM Tris-HCl (pH 7.2) containing 50% (v/v) sterile glycerol until required. The heme domain of the A264E mutant form of flavocytochrome P450 BM3 was also prepared in the same manner and as described previously.<sup>18</sup>

Prior to use in laser flash experiments, heme domain was exchanged into 100 mM potassium phosphate (pH 7.0) by dialysis at 4 °C. Buffers were made anaerobic by extensive bubbling with oxygen-free nitrogen, prior to incubation in an anaerobic glove box (Belle Technology, Portesham, U.K.), with oxygen levels maintained at  $< 2 \text{ ppm}$ . For laser photoexcitation experiments, 1 mL samples of BM3 heme domain ( $4\text{--}6 \mu\text{M}$  in 100 mM potassium phosphate, pH 7.0 for data collection over time bases of  $> 1 \text{ ms}$  or  $25 \mu\text{M}$  for data collection over time bases of

- (9) Murataliev, M. B.; Feyereisen, R.; Walker, F. A. *Biochim. Biophys. Acta* **2004**, *1698*, 1–26.  
 (10) Porter, T. D.; Kasper, C. B. *Proc. Natl. Acad. Sci. U.S.A.* **1985**, *82*, 973–977.  
 (11) Munro, A. W.; Leys, D.; McLean, K. J.; Marshall, K. R.; Ost, T. W.; Daff, S.; Miles, C. S.; Chapman, S. K.; Lysek, D. A.; Moser, C. C.; Page, C. C.; Dutton, P. L. *Trends Biochem. Sci.* **2002**, *27*, 250–257.  
 (12) Noble, M. A.; Miles, C. S.; Chapman, S. K.; Lysek, D. A.; Mackay, A. C.; Reid, G. A.; Hanzlik, R. P.; Munro, A. W. *Biochem. J.* **1999**, *339*, 371.  
 (13) Munro, A. W.; Daff, S.; Coggins, J. R.; Lindsay, J. G.; Chapman, S. K. *Eur. J. Biochem.* **1996**, *239*, 403.  
 (14) Miles, J. S.; Munro, A. W.; Rospendowski, B. N.; Smith, W. E.; McKnight, J.; Thomson, A. J. *Biochem. J.* **1992**, *288*, 503.

- (15) Hazzard, J. T.; Govindaraj, S.; Poulos, T. L.; Tollin, G. *J. Biol. Chem.* **1997**, *272*, 7922.  
 (16) Orii, Y. *Biochemistry* **1993**, *32*, 11910–11914.  
 (17) Daff, S.; Chapman, S. K.; Turner, K. L.; Holt, R. A.; Govindaraj, S.; Poulos, T. L.; Munro, A. W. *Biochemistry* **1997**, *36*, 13816–13823.  
 (18) Girvan, H. M.; Marshall, K. R.; Lawson, R. J.; Leys, D.; Joyce, M. G.; Clarkson, J.; Smith, W. E.; Cheesman, M. R.; Munro, A. W. *J. Biol. Chem.* **2004**, *279*, 23274–23286.

<1 ms) were excited using the third harmonic (355 nm) of a Q-switched Nd:YAG laser (Brilliant B, Quantel) in a sealed 1 mL quartz cuvette of 1 cm path length. The energy output of each laser pulse was up to 200 mJ, and pulses were 6–8 ns in duration. Other components of the various reaction mixtures used were pyridine nucleotide coenzymes (NADH, NADPH in the range from 0 to 1 mM), substrate *N*-palmitoylglycine (NPG, used at a final concentration of 50  $\mu$ M and having a  $K_d$  of 0.26  $\mu$ M),<sup>19</sup> and carbon monoxide (CO, used across the concentration range from 0 to 975  $\mu$ M, where the latter is saturating in solution at atmospheric pressure and 298 K).<sup>20</sup> Spectral transients were recorded at 340 nm [ $\Delta\epsilon_{340} = 6210 \text{ M}^{-1} \text{ cm}^{-1}$  for the oxidation of NAD(P)H to NAD(P)<sup>+</sup>], at 418 nm (absorbance maximum for the Soret band of low-spin BM3 heme domain;  $\epsilon_{418} = 95\,000 \text{ M}^{-1} \text{ cm}^{-1}$ ),<sup>12</sup> and at 450 nm (absorbance maximum for the BM3 Fe<sup>II</sup>–CO complex;  $\Delta\epsilon_{450-490} = 91\,000 \text{ M}^{-1} \text{ cm}^{-1}$  for the difference spectrum generated by subtraction of the spectrum for ferrous [Fe<sup>II</sup>] P450 from that for its Fe<sup>II</sup>–CO complex).<sup>21</sup> Parallel experiments were performed for enzyme samples in the absence of CO at these wavelengths and also at 390 nm (near the absorption maximum of the substrate-bound form, and at a wavelength which shows a substantial increase in absorption on reduction of the P450 heme iron from the ferric to the ferrous form) (Figure 1). Data collection was made using an Applied Photophysics LKS-60 flash photolysis instrument with the detection system at right angles to the incident laser beam. The probe light (150 W xenon lamp) was passed through a monochromator before and after passage through the sample. Absorbance changes were measured using a photomultiplier tube, and kinetic transients were typically collected over 50 ms. For measurements over faster timescales (typically <1 ms), the output of the xenon arc lamp was pulsed using a xenon arc pulser (Applied Photophysics), and transients were measured using an Infiniium oscilloscope model no. 54830B (Agilent Technologies). Absorbance spectra were measured before and after laser photoexcitation by transferring the cuvette to a Cary 50 UV–vis spectrophotometer (Varian) and recording data between 300 and 800 nm. All other spectral measurements for enzyme quantification and for establishing features of BM3 in ferric substrate-free and substrate-bound forms, the ferrous state, and in the Fe<sup>II</sup>–CO complex were also performed using a Cary 50 UV–vis spectrophotometer, either on the bench or under anaerobic conditions in a glove box (Belle Technology, Portesham, U.K. for the ferrous enzyme).

Data from photoexcitation experiments were analyzed and fitted to appropriate exponential functions using ProKin software (Applied Photophysics). All spectral and single-wavelength data were transferred to SigmaPlot 9.0 or Origin (Microcal) for further analysis. Absorption transients accompanying formation of the P450 BM3 heme domain Fe<sup>II</sup>–CO complexes fitted accurately to a standard double-exponential function, and rates for each phase ( $k_{\text{obs}}$ ) were plotted versus the concentration of other ligands/substrates varied for any set of experiments (NPG, carbon monoxide, or NAD(P)H). For experiments in which carbon monoxide concentration was varied, a hyperbolic dependence of the rate constant for formation of the Fe<sup>II</sup>–CO complex on CO concentration was observed. Data were fitted to a hyperbolic function to obtain estimates for the apparent limiting rate constant for Fe<sup>II</sup>–CO complex formation ( $k_{\text{lim}}$ ) and for the apparent dissociation constant for the Fe<sup>III</sup>:CO noncovalent complex.

*N*-Palmitoylglycine was synthesized according to the method described,<sup>19</sup> and binding of NPG was observed to induce a substantial shift in the P450 BM3 heme domain heme iron spin-state equilibrium from low-spin toward high-spin, confirming type I (substrate-like) binding to the P450. Bacterial growth media (Tryptone, yeast extract) were from Melford Laboratories (Ipswich, Suffolk, U.K.). All other

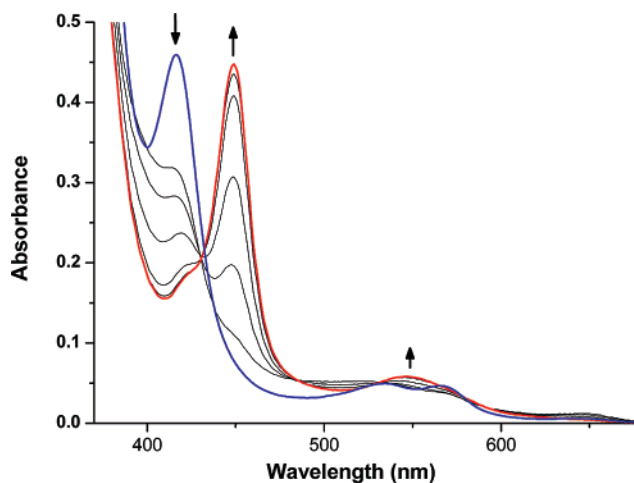


**Figure 2.** Conversion of ferric BM3 heme domain to the Fe<sup>II</sup>–CO complex by laser excitation of NADPH. The figure shows the progressive formation of the BM3 Fe<sup>II</sup>–CO adduct at 450 nm following laser excitation of 500  $\mu$ M NADPH in a solution containing 5  $\mu$ M BM3 heme domain and in the presence of a saturating (975  $\mu$ M) concentration of carbon monoxide. Spectra are shown prior to laser irradiation (blue spectrum) and after 1, 10, 20, 30, 40, and 50 laser flashes. The final spectrum (indicating near-complete formation of the thiolate-coordinated Fe<sup>II</sup>–CO complex at 450 nm) is shown in red. Arrows indicate the direction of spectral shifts at key wavelengths on conversion of the ferric enzyme to the Fe<sup>II</sup>–CO heme complex. A Soret shift from 418 to 450 nm is observed for the Fe<sup>II</sup>–CO complex, and there is development of an absorption band in the visible region at 548 nm. Minor spectral deviations from an isosbestic point between the Soret maxima may reflect altered contributions from NADPH coenzyme on its laser-induced oxidation.

reagents were from Sigma Aldrich (Poole, Dorset, U.K.) and were of the highest grade available.

## Results

### Laser-Induced Formation of the BM3 Fe<sup>II</sup>–CO Complex.

In preliminary experiments, we investigated whether laser flash photoexcitation of NAD(P)H was able to effect formation of the P450 BM3 heme domain Fe<sup>II</sup>–CO complex, starting from a mixture of ferric enzyme, CO, and NAD(P)H. Figure 2 shows spectral changes for an anaerobic mixture of BM3 heme domain (5  $\mu$ M) and 500  $\mu$ M NADPH, in the presence of 975  $\mu$ M CO (i.e., saturating at 25 °C and 1 atm).<sup>20</sup> Spectra are shown both before and following successive pulses of laser excitation at 355 nm. The Soret band at 418 nm (reporting on the ferric form of the enzyme) decreases upon laser excitation, as does the spectral contribution from reduced coenzyme absorption at 340 nm. A new species appears at 450 nm, reflecting formation of the reduced (Fe<sup>II</sup>) CO complex of the heme domain.<sup>21</sup> As illustrated in Figure 2, the conversion of BM3 heme domain to its P450 Fe<sup>II</sup>–CO complex is nearly complete following ~50 laser flashes, and there is negligible formation of the P420 Fe<sup>II</sup>–CO species with Soret absorption maximum close to 420 nm. The P420 form is associated with inactivated enzyme and can arise through protonation of the cysteine thiolate resulting in proximal coordination of the heme iron by cysteine thiol.<sup>22</sup> It is often difficult to avoid formation of a small amount of P420 enzyme following chemically (sodium dithionite) mediated heme iron reduction and bubbling with carbon monoxide gas.<sup>23</sup> Thus, the absence of any notable amount of P420 enzyme

(19) Haines, D. C.; Tomchick, D. R.; Machius, M.; Peterson, J. A. *Biochemistry* **2001**, *40*, 13456–13465.

(20) Cargill, R. *Carbon Monoxide*; Pergamon: Oxford, 1990; Vol. 43.

(21) Omura, T.; Sato, R. *J. Biol. Chem.* **1964**, *239*, 2370.

(22) Perera, R.; Sono, M.; Sigman, J. A.; Pfister, T. D.; Lu, Y.; Dawson, J. H. *Proc. Natl. Acad. Sci. U.S.A.* **2003**, *100*, 3641–3646.

(23) Munro, A. W.; Lindsay, J. G.; Coggins, J. R.; Kelly, S. M.; Price, N. C. *Biochim. Biophys. Acta* **1996**, *1296*, 127–137.



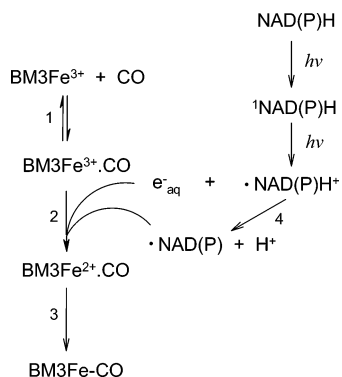


**Figure 3.** Scheme for formation of reductant products from photoexcitation of NAD(P)H and for the conversion of ferric BM3 heme domain to its Fe<sup>II</sup>-CO complex. On the right-hand side of the scheme, the excitation of NAD(P)H by laser irradiation ( $h\nu$ ) at 355 nm is assumed to be a two-photon event, with the formation of the singlet state of NAD(P)H [presented as <sup>1</sup>NAD(P)H] prior to the ejection of an aqueous electron ( $e_{\text{aq}}^-$ ) and formation of the <sup>•</sup>NAD(P)H<sup>+</sup> radical, which is then deprotonated to form <sup>•</sup>NAD(P) radical. The deprotonation of <sup>•</sup>NADH<sup>+</sup> to <sup>•</sup>NAD radical occurs with a rate constant of  $3.6 \times 10^6 \text{ s}^{-1}$  (step 4) (refs 16 and 24). On the left-hand side of the scheme, a rapid equilibrium binding of CO to the ferric (Fe<sup>3+</sup>) P450 BM3 heme domain is shown (step 1). The CO has no affinity for the ferric iron but instead populates one or more sites within the P450. Reduction of the P450 to its ferrous (Fe<sup>2+</sup>) state is achieved following laser excitation of NAD(P)H and as a consequence of the interaction of the P450 with either an aqueous electron or the <sup>•</sup>NAD(P) radical (step 2,  $k_{\text{obs}} \sim 14\,000 \text{ s}^{-1}$ ). The relocation of CO to a higher affinity site on the ferrous heme iron results in formation of the Fe<sup>II</sup>-CO complex (BM3Fe-CO) (step 3,  $k_{\text{im}} = 1770 \text{ s}^{-1}$  for NPG-free enzyme with NADH as reductant).

indicates that reduction of the heme domain using the laser photoexcitation method maintains the integrity of the heme binding site and that the proximal ligand remains as the native thiolate form.<sup>22</sup>

CO binds exclusively to the ferrous heme iron in the P450 enzyme. Thus, excitation of NADPH results in direct electron transfer to the ferric heme iron of BM3, a process which did not occur in previous studies of BM3 reduction involving photolysis of 5-deazariboflavin. According to Czochralska and Lindqvist, laser irradiation of NADH results in the ejection of a hydrated electron ( $e_{\text{aq}}^-$ ) and formation of the NAD<sup>•</sup> radical, as illustrated in Figure 3.<sup>24</sup> Both products are putative reductants of the P450 heme, although the  $e_{\text{aq}}^-$  ( $-2.9 \text{ V}$ ) has a substantially more negative reduction potential than the NAD<sup>•</sup> radical ( $-0.92$  to  $-0.94 \text{ V}$ ).<sup>25–27</sup> Evidently, the 355 nm irradiation of NADPH also facilitates  $e_{\text{aq}}^-$  release and rapid reduction of the BM3 heme iron. Carbon monoxide can then coordinate to the ferrous iron to produce the Fe<sup>II</sup>-CO complex with Soret maximum at 450 nm. Under aerobic conditions there was negligible formation of the 450 nm peak after excitation, suggesting electron transfer from NADPH to BM3 cannot proceed efficiently in the presence of saturating levels of oxygen. However, absorbance at 340 nm from NADPH decreased to almost the same level as was observed under anaerobic conditions following laser irradiation (data not shown). This illustrates that photoexcitation of NADPH still occurs under aerobic conditions. These findings are in agreement with those of Orii, which demonstrated that the  $e_{\text{aq}}^-$

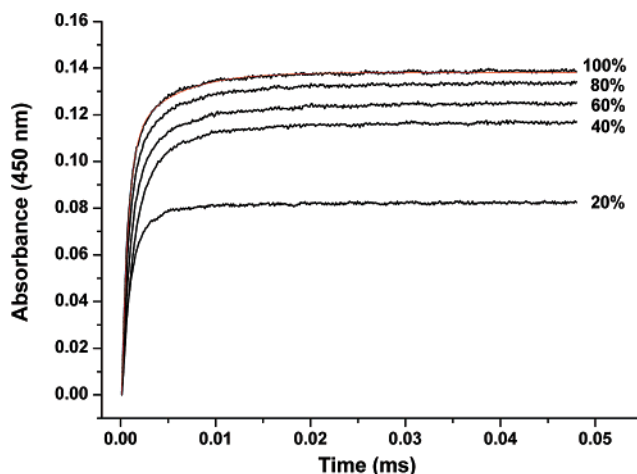


**Figure 4.** Typical reaction transients describing P450 BM3 heme domain Fe<sup>II</sup>-CO complex formation. Typical reaction transients at 450 nm are shown for the NADH-dependent formation of the Fe<sup>II</sup>-CO complex of BM3 heme domain. NADH ( $100 \mu\text{M}$ ) was irradiated as described in the Experimental Methods. Data were collected at 450 nm over 50 ms at the indicated concentrations of CO (expressed as percentage of saturation in solution, where  $975 \mu\text{M}$  represents 100% saturation). An exemplary biphasic fit (red) to the reaction progress curve is shown in the case of the transient recorded at 100% CO.

is a rapid reductant of dioxygen and that molecular oxygen can remove the electron from NAD<sup>•</sup> radical to form the superoxide anion.<sup>16</sup>

**Photoexcitation of Both NADH and NADPH Facilitates BM3 Heme Domain Reduction and Fe<sup>II</sup>-CO Complex Formation.** In parallel experiments, we established that NADH supported BM3 heme domain reduction and formation of the Fe<sup>II</sup>-CO complex with similar efficiency to that observed with NADPH. To determine rates of Fe<sup>II</sup>-CO complex formation, we followed development of absorbance at 450 nm on a microsecond time scale. Typical reaction transients for the NADPH-dependent reactions are shown in Figure 4. Reaction transients were described accurately by biphasic expressions. At a saturating CO concentration in solution ( $975 \mu\text{M}$ ), the fast phase rates of Fe<sup>II</sup>-CO complex formation were  $\sim 1350 \text{ s}^{-1}$  in the case of both NADH and NADPH ( $500 \mu\text{M}$ ). There was no apparent dependence of reaction rate on either coenzyme concentration in the range  $50\text{--}500 \mu\text{M}$ .

The lack of effect of coenzyme concentration on reaction rate suggests that CO binding to the heme was rate-limiting (as opposed to electron transfer from photoexcitation of the coenzymes). To explore this aspect further, we measured the rates of Fe<sup>II</sup>-CO complex formation across a range of CO concentrations from 0 to  $975 \mu\text{M}$  following photoexcitation of NAD(P)H. The rate of Fe<sup>II</sup>-CO complex formation at 450 nm was dependent on CO concentration, as illustrated in Figure 5A for data collected with both NADPH and NADH as electron donors. The hyperbolic dependence is consistent with a rate-limiting CO association with the ferrous heme iron. Both phases of the biphasic transients showed a similar dependence on CO concentration. Apparent dissociation constants ( $K_{\text{d app}}$  values) were obtained from hyperbolic fits of both the fast phase and slow phase rate constants versus CO concentration (Table 1). We infer that these values relate to a noncovalent Fe<sup>III</sup>:CO complex (see Figure 3), although we cannot rule out at this stage a prebinding step for CO to the ferrous enzyme prior to iron coordination. These  $K_{\text{d app}}$  values were  $323 \pm 53$  and  $600 \pm$

(24) Czochralska, B.; Lindqvist, L. *Chem. Phys. Lett.* **1983**, *101*, 297–299.

(25) Anderson, R. F. *Biochim. Biophys. Acta* **1980**, *590*, 277–281.

(26) Buxton, G. V.; Greenstock, C. L.; Helman, W. P.; Ross, A. B. *J. Phys. Chem. Ref. Data* **1988**, *17*, 513–531.

(27) Farrington, J. A.; Land, E. J.; Swallow, A. J. *Biochim. Biophys. Acta* **1980**, *590*, 273–276.

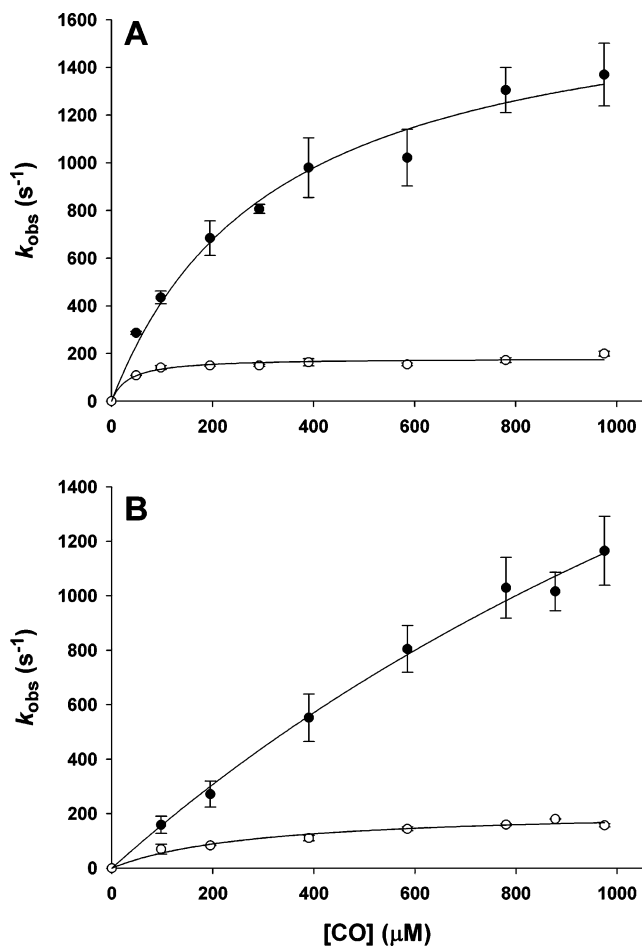


**Figure 5.** Dependence of the rate of formation of the P450 BM3 heme domain  $Fe^{II}$ -CO complex on the concentration of carbon monoxide. Reactions were carried out as described in the Experimental Methods for both the substrate-free (panel A) and NPG-bound (panel B) forms of the P450 BM3 heme domain. All reaction transients were biphasic. Data are shown (with error bars showing the standard deviation) for rates of the fast phase (filled circles) and the slow phase (open circles) across the range of CO concentrations tested and with NADH as the reductant. NADH concentration was maintained at  $100 \mu M$  in all experiments. Data are fitted to hyperbolic expressions. The relevant  $k_{lim}$  and apparent  $K_{d(CO)}$  values are reported in Table 1.

**Table 1.** Kinetic and Equilibrium Binding Parameters Associated with CO Binding to P450 BM3 Heme Domain

		NADH		NADPH	
		substrate-free	+NPG	substrate-free	+NPG
rate 1	$k_{lim} (s^{-1})$	$1770 \pm 115$	$3036 \pm 287$	$1996 \pm 327$	$7133 \pm 1869$
	$K_{d(CO)} (\mu M)$	$323 \pm 53$	$1404 \pm 204$	$600 \pm 200$	$3378 \pm 109$
rate 2	$k_{lim} (s^{-1})$	$180 \pm 8$	$216 \pm 17$	$283 \pm 11$	$361 \pm 39$
	$K_{d(CO)} (\mu M)$	$33 \pm 10$	$277 \pm 67$	$349 \pm 35$	$739 \pm 155$

$200 \mu M$  for NADH and NADPH, respectively, for data analyzed from the fast phase of the biphasic reaction process. Limiting rate constants ( $k_{lim}$  values) for formation of the  $Fe^{II}$ -CO complex were  $1996 \pm 327 s^{-1}$  for the fast phase and  $283 \pm 11 s^{-1}$  for the slow phase with NADPH as donor. Corresponding rate constants with NADH as the electron donor were similar at  $1770 \pm 115$  and  $180 \pm 8 s^{-1}$  (Table 1).

As seen in Figure 1, there is a substantial decrease in the absorption near the Soret peak (positioned at  $418 nm$ ) as the enzyme is converted from its ferric to ferrous form and also as it is converted from the ferric form to the ferrous-CO complex.

The maximal absorbance difference between the ferric and ferrous states of the enzyme is seen at  $\sim 422 nm$  (Figure 1, inset). To investigate further the kinetics of  $Fe^{II}$ -CO complex formation at a wavelength distinct from  $450 nm$ , we examined the absorption decrease at both  $418$  and  $422 nm$  for substrate-free enzyme with photoexcited NADH ( $100 \mu M$ ) as reductant. Reaction transients remained biphasic at these wavelengths, with rates comparable to those observed at  $450 nm$  (e.g.,  $1220$  and  $310 s^{-1}$  at  $422 nm$ ).

**Kinetics of  $Fe^{II}$ -CO Complex Formation in Substrate-Bound BM3 Heme Domain.** Substrate binding to P450 BM3 heme domain results in the perturbation of the heme iron spin-state equilibrium in favor of the high-spin form, with a substantial shift in the heme optical spectrum (Figure 1). The binding of fatty acid substrates also leads to an increase in heme iron reduction potential (from  $-427$  to  $-289 mV$  in the case of arachidonic acid) that triggers electron transfer from the FMN cofactor in the natural catalytic cycle of the flavocytochrome.<sup>17,28</sup> The extent of conversion of spin-state equilibrium is highly substrate-dependent for P450 BM3. *N*-Palmitoylglycine (NPG) is one of the best substrates for BM3 and effects an almost complete conversion to the high-spin form at saturation. Binding of NPG substrate leads to the BM3 Soret band shifting to  $390 nm$  (Figure 1). Binding of NPG would be expected to make BM3 heme iron reduction even more thermodynamically favorable. However, NPG also occupies active site volume and could obscure access of CO to the ferrous BM3 heme iron. Moreover, the atomic structures of palmitoleate- and NPG-bound heme domains are distinct to that of the ligand-free enzyme, suggesting either substrate-induced conformational rearrangement of the P450 or stabilization of the relevant conformer by substrate binding.<sup>18,29,30</sup> To evaluate effects of substrate (NPG) binding on the rate of  $Fe^{II}$ -CO complex formation, we repeated laser photoexcitation studies and examined the NAD(P)H and CO concentration dependence of reaction rates, as done for the substrate-free enzyme. Reaction transients for  $Fe^{II}$ -CO complex formation at  $450 nm$  remained biphasic, and similar overall rates for the formation of the  $Fe^{II}$ -CO complex were observed in the presence and absence of NPG. As with substrate-free enzyme, observed rates obtained with NPG-bound BM3 were independent of NAD(P)H concentration ( $50 \mu M$  to  $1 mM$ ) but dependent on CO concentration. However, there is an apparent weaker binding of CO to the heme domain protein (likely the ferric form) in the presence of NPG. This is particularly clear from the outward shift in the hyperbolic curve fitted through the data points for  $k_{obs}$  for the fast phase of  $Fe^{II}$ -CO complex formation (see Figure 5B). Apparent saturation with CO was not reached in the accessible range to  $975 \mu M$ , and this is reflected both in the inflated apparent  $K_d$  values for CO and also in the much larger errors associated with the data fitting for both the  $k_{obs}$  and  $K_d$  values (Table 1).

**Analysis of the Formation of the  $Fe^{II}$ -CO Complex in a Conformationally Constrained A264E Mutant.** In view of the biphasic nature of reaction transients obtained for CO binding to BM3 heme domain reduced by photoexcited NAD(P)H, we also examined CO binding to the A264E mutant heme

(28) Ost, T. W. B.; Miles, C. S.; Munro, A. W.; Murdoch, J.; Reid, G. A.; Chapman, S. K. *Biochemistry* **2001**, *40*, 13421-13429.

(29) Li, H.; Poulos, T. L. *Nat. Struct. Biol.* **1997**, *4*, 140-146.

(30) Joyce, M. G.; Girvan, H. M.; Munro, A. W.; Leys, D. *J. Biol. Chem.* **2004**, *279*, 23287-23293.

domain in the same photoexcitation reaction. Our previous structural studies of this mutant showed that it adopted a conformation typical of the substrate (fatty acid)-bound form of the wild-type BM3 in both the presence and absence of substrate.<sup>30</sup> Thus, A264E appears to be a conformationally “locked” mutant and one which could shed light on the possible relevance of conformational equilibria to the biphasic nature of the CO binding kinetics observed in the wild-type BM3 heme domain. At saturating CO concentration, we found that reaction transients for Fe<sup>II</sup>–CO complex formation in the A264E heme domain remained biphasic and that rates of CO association to the ferrous heme iron were slightly slower than for the wild-type BM3 (e.g., 730 and 90 s<sup>-1</sup> using NADH at 100 μM, with CO at 950 μM). The slower rate of Fe<sup>II</sup>–CO complex formation in the A264E mutant might be attributable to steric hindrance in the binding of CO to the ferrous heme. Atomic structural studies of the substrate-free A264E heme domain showed that the bulky glutamate 264 side chain occupies either of two positions in the protein. One of these is as the sixth ligand to the P450 heme iron. The other is interacting with the side chain of active site residue phenylalanine 87 and so obscuring somewhat the active site access channel to the heme iron.<sup>30</sup> Amplitudes of the A264E Fe<sup>II</sup>–CO complex formation reaction transients were also only ~30% of those for the wild-type BM3, consistent with the partial occupancy of the ferric heme iron by glutamate 264 as the sixth ligand.<sup>18</sup>

**Analysis of BM3 Heme Reduction Kinetics by Coenzyme Photolysis in the Presence and Absence of CO.** In all the NAD(P)H photoexcitation experiments described above, rapid absorption decreases were observed at 340 nm (i.e., at the absorption peak for the reduced coenzymes) after each laser flash, consistent with previous data and with the rapid laser-mediated oxidation of NAD(P)H.<sup>16</sup> The rate of this process was ~8 × 10<sup>6</sup> s<sup>-1</sup>, substantially faster than the apparent rate of Fe<sup>II</sup>–CO complex formation. These data indicate that release of a hydrated electron from NAD(P)H occurs >10<sup>3</sup>-fold faster than the limiting rate (*k*<sub>lim</sub>) for formation of the Fe<sup>II</sup>–CO complex. To demonstrate unequivocally that reduction of BM3 heme iron from ferric to ferrous occurs at a rate substantially faster than the apparent *k*<sub>lim</sub> for the formation of the Fe<sup>II</sup>–CO complex, we performed laser photoexcitation reactions over faster time scales, as described in the Experimental Methods.

With the laser flash instrument set up for more rapid data acquisition (i.e., less than 1 ms), we analyzed data at 390, 422, and 450 nm for substrate-free BM3 heme domain in both the presence (950 μM) and absence of CO, with NADH used as the reductant. With lower signal-to-noise ratio in this experimental mode, we increased both enzyme (25 μM) and NADH concentration (500 μM) 5-fold. Transients were collected for up to 5 ms to establish whether a faster enzyme reduction step could be observed prior to binding of CO to the heme iron. In the CO-saturated enzyme (and at each of the wavelengths tested), the reaction transients were now clearly triphasic, with a much faster first phase than previously observed. The remaining two phases were comparable to those observed previously for the formation of the Fe<sup>II</sup>–CO complex using the slower time frame analysis (e.g., *k*<sub>1</sub> = 14 000, *k*<sub>2</sub> = 3500, and *k*<sub>3</sub> = 380 s<sup>-1</sup> at 450 nm). To confirm that the fast phase was indeed due to the NADH-dependent reduction of the enzyme, experiments were repeated in absence of CO. In all cases, the

reaction transients became monophasic with rate constants consistent with the fast phase extracted from the triphasic transients observed in the presence of CO (e.g., 13 500 s<sup>-1</sup> at 390 nm). These data are therefore consistent with a rapid monophasic enzyme reduction process following photoexcitation of NAD(P)H, followed by a biphasic process of CO association with the ferrous heme iron. At ~14 000 s<sup>-1</sup>, P450 heme reduction by NAD(P)H photoexcitation is several-fold faster than both the “natural” rate of flavin-to-heme electron transfer in the enzyme (223 s<sup>-1</sup> at 25 °C) and the maximal rate reported for steady-state fatty acid (arachidonate) hydroxylation (285 s<sup>-1</sup> at 30 °C).<sup>12,13</sup>

## Discussion

We have reported a novel laser flash photoexcitation method for the rapid reduction of the heme domain of cytochrome P450 BM3. Irradiation of NAD(P)H leads to the release of an aqueous electron and to fast reduction of the P450 BM3 heme iron at a rate of ~14 000 s<sup>-1</sup>. We have used this method of reducing the heme domain to analyze binding of CO to the ferrous heme iron in the absence and presence of the tight-binding substrate NPG. Our studies indicate a biphasic transient for CO binding to the ferrous heme. The rate of formation of the Fe<sup>II</sup>–CO complex is hyperbolically dependent on the CO concentration, and the kinetic behavior is consistent with a rapid equilibrium CO binding step (that occurs prior to the laser excitation), followed by fast electron transfer on laser irradiation, and then a relatively slow coordination of CO to the ferrous form of the P450 heme iron (Figure 3). Thus, reduction of the heme iron to its ferrous form following laser irradiation of NAD(P)H enables relocation of CO from proximal lower affinity site(s) in the P450 protein to occupy the high-affinity site on the ferrous heme iron and to form the stable Fe<sup>II</sup>–CO complex. The biphasic nature of the CO binding kinetics might be explained by (i) distinct low-affinity CO sites in the ferric BM3 heme domain or (ii) different conformational states of the P450 enzyme. Crystallographic studies of the BM3 heme domain have revealed two distinctive conformations in the substrate-free (SF) and substrate-bound (SB) forms.<sup>29,31</sup> More recent studies have indicated that an A264E point mutant also adopted the SB conformation, whether or not substrate was bound.<sup>30</sup> This suggests that both SF/SB conformations are accessible to the substrate-free enzyme. Further structural data have also indicated a third conformation with more open active site access in both wild-type and A264E mutants.<sup>18,30</sup> Thus, structural plasticity of the P450 enzyme might give rise to coexisting and distinctive conformations of the P450 that could result in altered CO binding kinetics.

Complex kinetics for the binding of CO to P450 enzymes have been reported previously. In studies of the binding of CO to ferrous BM3 heme domain (following photolysis of the Fe<sup>II</sup>–CO adduct), complex bimolecular and geminate CO rebinding kinetics were observed, the origin of which was suggested to arise from different conformational states of the P450.<sup>32</sup> The binding of fatty acids gives rise to monophasic bimolecular CO binding kinetics, a behavior which has been attributed to decreased protein conformational heterogeneity.<sup>32</sup> In P450cam

(31) Ravichandran, K. G.; Boddupalli, S. S.; Hasemann, C. A.; Peterson, J. A.; Deisenhofer, J. *Science* **1993**, *261*, 731–736.

(32) McLean, M. A.; Yeom, H.; Sligar, S. G. *Biochimie* **1996**, *78*, 700–705.



(CYP101A1), biphasic second-order CO binding kinetics have been reported in both the presence and absence of camphor substrate.<sup>33</sup> Studies of the heme proteins myoglobin and hemoglobin have also indicated that CO binding kinetics are highly sensitive to protein conformational dynamics.<sup>34</sup> In the case of P450 BM3, there is also evidence for structural effects accompanying the spectroscopically silent association of CO with the ferric heme domain. In their studies of 5-deazariboflavin-mediated FMN reduction of the FMN–heme domain construct of P450 BM3, Hazzard et al. inferred that conformational changes that favor flavin-to-heme electron transfer occurred on binding CO within the ferric P450 active site pocket.<sup>15</sup> Also, Murataliev and Feyereisen have reported that CO stimulates FMN-dependent electron transfer to cytochrome *c* in the presence of fatty acid substrate. Thus, CO association can impact on the kinetics of electron transfer through the reductase domain of the enzyme.<sup>35</sup> While the origins of these effects remain unclear, it is possible that they arise from structural effects induced by CO binding to the heme domain.<sup>35</sup> Thus, preceding data on the interactions of CO with P450 BM3 provide evidence for binding of this ligand to the ferric P450 and also suggest structural perturbations may result from interactions that CO makes with the heme domain that do not involve direct heme iron coordination.<sup>15</sup> Consistent with these ideas, we propose that conformational heterogeneity in the BM3 heme domain and (possibly) occupancy of low-affinity sites for CO in the ferric (or possibly ferrous) P450 protein give rise to the biphasic kinetics of Fe<sup>II</sup>–CO complex formation observed in NAD(P)H laser irradiation studies.

While we ascribe heme iron reduction to aqueous hydrated electrons released from photoexcitation of NAD(P)H, we cannot at this stage rule out some contribution to heme reduction from the NAD(P)<sup>•</sup> radical. The NAD<sup>•</sup> radical has been reported to

be a reductant for cytochrome *c* and to form rapidly by deprotonation of <sup>•</sup>NAD(P)H<sup>+</sup>, the other primary product of photolysis of NAD(P)H (Figure 3). The fact that reduction of the heme iron by NAD(P)H photolysis is rapid and monophasic (in the absence of CO) suggests that aqueous hydrated electrons may be the primary reductants and that the biphasic kinetics observed for the slower CO binding process is not related to the influence of a second reductant species.

## Conclusions

We have reported (i) a novel application of NAD(P)H photoexcitation chemistry as a route to the rapid reduction of cytochrome P450 BM3 and (ii) exploitation of the method for the analysis of CO binding. Irradiation of NAD(P)H facilitates rapid reduction of the ferric heme iron ( $\sim 14\,000\text{ s}^{-1}$ ), and this technique is thus suitable for analysis of the formation and interconversion of oxy intermediates in the P450 catalytic cycle, particularly given the availability of mutants that stabilize the ferrous–oxy form of the P450.<sup>28</sup> Previous studies of Oriei involving photoexcitation of NADH and reduction of cytochrome *c* have established that the photochemistry is feasible at low oxygen concentrations (a requirement for studies of the P450 reaction cycle). Direct reduction of the P450 heme using nicotinamide coenzyme photochemistry bypasses limitations encountered with the photoreductant 5-deazariboflavin, which directly reduces the FMN cofactor but not the P450 heme iron.<sup>15</sup> Our approach is thus promising for detailed spectroscopic and kinetic studies of the P450 reaction cycle, studies that we are now pursuing.

**Acknowledgment.** The authors thank the U.K. Biotechnology and Biological Sciences Research Council (BBSRC), the Royal Society, and the Leverhulme Trust (U.K.) for funding project grants supporting this study and for awards of Senior Research (A.W.M.) and Professorial Fellowships (N.S.S.).

(33) Tian, W. D.; Wells, A. V.; Champion, P. M.; DiPrimo, C.; Gerber, N.; Sligar, S. G. *J. Biol. Chem.* **1995**, *270*, 8673–8679.

(34) Austin, R. H.; Beeson, K. W.; Eisenstein, L.; Frauenfelder, H.; Gunsalus, I. C. *Biochemistry* **1975**, *14*, 5355–5373.

(35) Murataliev, M. B.; Feyereisen, R. *Biochemistry* **1996**, *35*, 15029–15037.

JA071355M